Cumulative Lognormal Distributions of Dose-Response vs. Dose Distributions

A. Brodsky
Science Applications International Corporation*
M/S SH2-1, 1410 Spring Hill Road, McLean, VA 22102.
and Georgetown University, Washington, DC 20007

ABSTRACT

A review of the author's findings over four decades will show that the lognormal probability density function can be fit to many types of positive-variate radiation measurement and response data. The cumulative lognormal plot on probability vs. logarithmic coordinate graph paper can be shown to be useful in comparing trends in exposure distributions or responses under differing conditions or experimental parameters. For variates that can take on only positive values, such a model is more natural than the "normal"(Gaussian) model. Such modeling can also be helpful in elucidating underlying mechanisms that cause the observed data distributions. It is important, however, to differentiate between the cumulative plot of a dose distribution, in which successive percentages of data are not statistically independent, and the plots of dose-response data for which independent groups of animals or persons are irradiated or observed for selected doses or dose intervals. While independent response points can often be best fitted by appropriate regression methods, the density functions for cumulative dose or concentration distributions must be fit by particular maximum likelihood estimates from the data. Also, as indicated in the texts by D. J. Finney and by R. O. Gilbert, for example, a simple plot of such data on available probability (or probit) vs. log scale graph paper will quickly show whether an adequate representation of the data is a lognormal function.

Processes that naturally generate lognormal variates are sometimes estimated by statistics that follow the lognormal straight line for a cumulative plot on a probability vs. log scale; on the other hand, sometimes the statistics of interpretation follow such a line only over a certain range. Reported examples of lognormal occupational exposure distributions include those in some facilities in which roundoff biases were removed for some years. However, for a number of exposure distributions at licensed facilities in the United States, the cumulative exposure distributions curved upward above about 1 rem, showing the pressure of the 5 rem limit in constraining the "natural" distribution of occupational exposure. The United Nations Scientific Committee (UNSCEAR) adopted this type of display in some of its reports. Kumazawa and associates (1981, 1982) fitted some of these distributions by a function named "the hybrid lognormal", which has been used to describe exposure distributions in Canada (Sont and Ashmore 1988). Examples of the suitability of the lognormal dose-response function for animal data on lethality and carcinogenesis have been reported earlier by the author. In 1998, the close representation of a lognormal fit to the excess absolute mortality from solid cancers was reported by the author for the Hiroshima-Nagasaki cohorts reported by UNSCEAR. The close representation of a two-stage model of carcinogenesis by families of lognormal functions has also been reported. In 1999, the author showed that the deviation (in the low range) from lognormality of plutonium in urine measured by fission track analysis can be explained as the result of convoluting observed lognormal human sample data with the randomly varying and also lognormally distributed tracks of the subtracted reagent blanks. The sum or difference of two lognormally distributed variates is not lognormal; yet, in the higher range of interpreted plutonium activity in urine samples – well above the range of variation of the blanks — the "true" lognormality of excreted plutonium can be exhibited. Thus, reasons for the departure from an actual lognormal distribution of a fundamental quantity of interest can often be explained by examining the actual measurements and calculations leading to the interpeted results. A sample of these phenomena, as observed by the author, are presented and discussed in this paper.

INTRODUCTION

Selected presentations of the author (1-12) will be reviewed to show the many potential advantages of considering the lognormal function in modelling: (a) the cumulative distributions of doses, exposures, or concentrations in various media; and (b) many of the biological acute and chronic responses as functions of radiation (or chemical) dose to tissue. Many other examples of the uses of the lognormal function in medicine, biology, economics, sociology and other sciences, and the mathematical properties the lognormal function and the estimation of its parameters, are presented comprehensively in major treatises (13-15). I believe that my earliest introduction to the lognormal probability density function, and the usefulness of the probability vs. log scale graph paper designed to provide a straight line for the cumulative plot of lognormal data, was in a course on industrial hygiene in the early 1960s by Professor T. F. Hatch. He was the first to present and describe mathematically the distribution of screened particle sizes as lognormal (16, 17). Having then a supply of lognormal graph paper readily available, I would begin to use its convenient log and % scales to plot other data that ranged over orders of magnitude, even when not expected to show the lognormal characteristics. However, I soon found that most of the dose distribution data, response data, and other random variables constrained to

have only positive values, was often best modelled and examined by the use of the lognormal function. More recently, excess absolute risk data for solid cancers in the Japanese atomic bomb survivor population, and the derived results of subtracting blank data from control population data on plutonium in urine, as measured by fission track analysis (FTA), have shown consistency with the lognormal model (10-12). In the FTA analysis, the interpreted amounts of plutonium in daily urines of a preliminary control population were initially found to deviate from lognormal in the low range, the usual straight line curving to the left at low concentrations (shown here later). As described in the SAMPLE EXHIBITS section, further examination showed that the curvature could be described by mathematically deriving the distribution function for the difference between what was found to be a lognormal track/24-hour control urine distribution and the lognormal simulated urine blank distribution. Thus, the "true" or actual distribution of daily plutonium excretion is lognormal, but the plutonium activity as "interpreted" by human subtraction of a random blank produces (artificial) negative quantities that skew the distribution to the left. However, it is important that, if statistical tests are to be made against the interpreted distributions (which might be all we have) rather than assumed normal or lognormal distributions, the distributions should be properly characterized mathematically for use in constructing the necessary decision and test criteria. Only a brief summary of these phenomena can be presented here. Further examples, and the author's derivation of probability density functions (pdfs) for the interpreted distributions (a derivation that can be adapted in general to other functional distributions) can be examined in the references cited.

DEFINITION OF LOGNORMAL PARAMETERS

The lognormal function as a pdf represents a distribution of random variates when the logarithms (either natural or common) of the variates are normally (Gaussian) distributed (13-15). Since the various references on mathematical properties and applications of the lognormal function use a variety of symbols, the main properties of the lognormal have been summarized and some of the definitions have been related in Reference 18. The paper uses symbols, basic definitions, and equations as in Reference 18. The probability scale, as shown in Figures 1 through 12, is marked so that the % indicated is the integral (times 100 to give percent) from negative infinity over the normal distribution up to the number of standard deviations from the mean, as marked on a corresponding "probit" (13) or linear scale. See, for example, Figure 12, where the % values marked on the left scale correspond to the probits (probit = 5 being set at the center of the distribution) on the right-hand scale. Finney (13) defined 5 probits to be in the center of the normal distribution of logarithms, for the convenience of biologists who would then not need to work with negative numbers in constructing straight line plots.

The form of the lognormal pdf may be given as:

$$p(x) = \{\exp[-(1n\ x - 1n\ \mu_g)^2/\sigma_g^2]\}/(2\pi)^{1/2}.\sigma_g \qquad \text{Eq.1}$$

where x is the variate that is lognormally distributed, lnx is the natural logarithm of x, μ_g is the median of x, $ln\mu_g$ is the mean value of lnx, and σ_g is the standard deviation of the (normal) distribution of ln x. A similar definition can be made in terms of logarithms to the base 10.

The cumulative probability distribution of ln x is:

$$p(\ln X) = \text{Probability}\ (\ln x \le \ln X) = \int_{\ln x=\ln 0\rightarrow-\infty}^{\ln x=\ln X} p(x)\, d(\ln x) \qquad \text{Eq. 2}$$

which upon differentiation of d(ln x) gives the cumulative probability distribution for x as a lognormal cumulative probability function:

$$F(x) = \text{Prob}\ (x \le X) = \int_{x\rightarrow 0}^{x=X} [p(x)/x]\, dx \qquad \text{Eq. 3}$$

The integral converges as x tends to zero; x must not be set equal to zero, since the pdf for the lognormal distribution of x, p(x)/x, is infinite at x = 0. However, in calculations the integral converges rapidly so that practical small values of x (perhaps only several standard deviations to the left of center) suffice to provide a stable F(x) function.

The relationship between the mean m of the lognormal population and the median m_g is:

$$\ln \mu = \ln \mu_g + \sigma_g^2/2 \qquad \text{Eq. 4}$$

and in terms of logarithms to the base 10 this Equation becomes:

$$\log_{10} (\mu/\mu_g) = 1.1513 (\log_{10} s_g)^2 \qquad \text{Eq. 5}$$

where s_g is termed the "standard geometric deviation", "geometric standard deviation", or "geometric mean standard deviation" in various texts. It is related to the standard deviation of ln x by:

$$\sigma_g = \ln s_g \qquad \text{Eq. 6}$$

The value of m_g (the median) can be estimated from a graphic plot of the % of sample data ≤ x, at each value of a sequence of x values on a logarithmic scale. A sample of about 40 data points can usually be plotted in minutes by simply adding the number of data values below or at each x value and calculating the percentage of the total number of data values. The median is then the value of x at which the fitted line (if the data are seen to be lognormal) crosses the 50% horizontal line. The value of s_g may also be estimated graphically within about five percent for well-fitting straight lines by taking ratios of the x values at 84.13% to 50%, or 50% to 15.8%, or an average of the two.

$$s_g = x(84.13\%)/x(50\%) = x(50\%)/x(15.87\%) \qquad \text{Eq. 7}$$

If the plotted cumulative points are independent of each other, as for independently exposed groups of animals in a response vs. dose study), then the parameters of the lognormal function can be estimated most precisely from a simple regression analysis (where variances in effect are constant with dose (not likely)) or from an appropriately weighted regression. However, for dependently plotted data, as in some dose distribution studies, the median and standard geometric deviation can be estimated from the sample with minimum variance by using maximum likelihood estimators (11, 12, 14). The maximum likelihood estimator of the median, as calculated from sample values x_i, (omitting any zero values) is:

$$\widehat{\ln \mu_g} = \{\Sigma_{i=1}^{i=N} (\ln x_i)\}/N, \qquad \text{Eq. 8}$$

which can be seen by algebraic manipulation to be the "geometric mean" of the sample. The maximum likelihood estimator of the standard deviation of ln x is:

$$\widehat{\sigma_g}^2 = \Sigma_{i=1}^{i=N} (\ln x_i - \ln\mu_g)^2/N, \qquad \text{Eq. 9}$$

from which an estimate of s_g can be calculated from Eq. 6. The "hats" (inverted Vs) over the estimated parameters in Equations 8 and 9 indicate that these equations provide estimates from finite data sets; the estimates might deviate to some degree from the underlying "true" parameters of the distribution. Values of the median and the standard geometric deviation will be the parameters most used in the following examples. A 95% interval about the median of a lognormal distribution can be estimated as μ_g times or divided by $s_g^{1.96}$.

SAMPLE EXHIBITS OF LOGNORMALLY DISTRIBUTED QUANTITIES

Cumulative Distributions of Dose, Concentration, or Other Quantities (Dependent Points)

Many distributions of occupational exposure plotted on "lognormal paper" have been observed by the author to be modelled well by using the lognormal function. In the early 1960s, a study of exposure distributions in various operations associated with a test reactor facility showed lognormality of annual employee exposures when film badge readings were no longer "rounded off" by some arbitrary *a priori* criteria (2). The author has observed consistent straight-line plots on lognormal paper of annual exposure distributions of employees in a medical institution under his surveillance (6). Figure 1 shows an example of the shapes of dose distributions from employees of all licensees of the U. S. Nuclear Regulatory Commission (NRC)(7). Although different categories of licensees are included in these data, and although sums of variates from different lognormally distributed populations are not, in general, lognormally distributed, these plots exhibit the lognormal cumulative distribution in the dose range below about 1 rem. These lines may be extrapolated to lower doses to estimate the low median exposure for NRC employees. On the other hand, at the range above 1 rem, the curves deviate from the lognormal line and bend upward. This upward deviation can possibly be interpreted as a deviation from the "normally" lognormal shape at higher levels as an effect of the "pressure" of the 5 rem annual limit. Kumazawa and associates fitted the lognormal and upward-curved shape by a hybrid lognormal function, which has been used in some United Nations Scientific Committee on Effects of Atomic Radiation (UNSCEAR)

reports to examine trends of exposure between nations and industries. The hybrid lognormal has also been used to study exposure distributions in Canada (19). Caution should be used so that presumed plotting of only arbitrarily-assumed positive readings does not distort trends in radiation protection. If protection has improved so that the lower-exposed employees who do not need to be involved in radiation areas are managed in a way that their doses are reduced, while the other employees are maintained at the same level of safety, plotting only "positive" readings could give the false impression that the median exposure of the workforce has increased (the observer would not likely know that some employees have been removed from the plot –see Figure 1). Of course, if an employee population is composed of groups having widely disparate exposures, their combined distribution might not exhibit a lognormal shape, but instead be bimodal, multi-modal, or otherwise different than lognormal.

Figures 2-4 show samples of the many distributions of elements and radionuclides in environmental, food, and tissue samples, examined in the era of more intense fallout from nuclear weapons tests, that usually were fit well by the lognormal function (4). Figure 2 shows distributions of naturally occurring elements in human tissue samples. Figure 3 compares the relative slopes and positions of plots of ^{90}Sr per gram of calcium, and per gram of bone, in human bone samples in the United States in 1964-65. This plot illustrates, through the parallel lines on the right, that the ratio between concentrations per gram calcium and per gram bone is constant with concentration level; thus, one measurement can be converted to another by a constant factor. The uptake of strontium within the concentration range in humans is not affected by the amount of calcium in bone. Comparison of the slopes (s_g values) between Figures 3 and 4 indicates that the variability of the strontium-90 concentrations in milk and in human bone is not much different than the variability in soil deposits throughout the United States. This indicates that not much additional variability in uptake by individuals is introduced by factors of cow uptake, milk excretion, and individual physiological processes. The lognormal distribution can be shown by mathematical derivation to be a natural outcome of a variate resulting from many multiplicative factors, each contributing a small proportion to the final observed quantity, just as a normal distribution is expected from the algebraic addition of many quantities (4, 18). The multiplicative factors in environmental radiation studies can be, for example, a product of the fraction of fallout incident on a given area of land, multiplied by the fraction of that ingested by cattle, multiplied by the fraction of the ingested amount reaching breast milk, multiplied by the fraction in breast milk taken by the farmer…— each factor a positive variate. Examination of the standard geometric deviations of the bone distributions of strontium-90 was helpful in assuring the soundness of an early policy of the U. S. Federal Radiation Council of assuming that no subgroup of a population would likely be more than three times the mean concentration (4).

Figure 5 shows the distribution in volumes of daily output of urine by a worker under diethylene, triamine, penta-acetic acid (DTPA) therapy for removal of plutonium from 1967-69, separated for comparison into two time intervals to examine consistency of output over time (5). This individual was diligent in bringing in almost a total collection of daily urines over a long period of time. (This figure has been previously published only in a progress report.) The shapes of the distributions for the two time intervals are consistent, except for the curvature to the left at the lower outputs in the later time interval.

Figure 6 shows the distribution of numbers of tracks from 75 simulated urine reagent blanks in a fission track analysis (FTA) process for measuring plutonium, projected to linear and to logarithmic track scales (11, 12). The choice of distribution function is obviously the lognormal and not the normal. In Figure 7, the (limited sample) distributions of tracks (corrected to 24-hour output) from FTA analysis of urines from two subpopulations that differ in median plutonium excretion are seen to provide a distribution closely fit by a lognormal function when pooled together. The pooled population is a preliminary construct to simulate a "control" set of urine plutonium excretion values approximating urine outputs from persons throughout the United States exposed to plutonium only from fallout.. (These data are not necessarily to be taken as representative of any long-term analytical process to be used for an official purpose, but are presented here for illustrating certain characteristics of analytical methods.) The data in both Figure 6 and Figure 7 are comprised of positive (non-negative) variates, the natural outcome of the fundamental measurement process. However, as is often the case when the values of randomly fluctuating blank measurements, or even blank averages ("well-known" blanks), are subtracted from low-level random measurements of samples (or even radiation exposure rates), some results yield negative numbers. These negative results are artifacts of the human manipulation of the basic measurement data, and do not necessarily show that the resulting distribution, termed here the "interpreted" result distribution, is indicative of the deviation of the underlying distribution from a lognormal (or perhaps other underlying "true" distribution). The interpreted distribution of the control urine outputs is shown in Figure 8 as triangles, in comparison with two distributions mathematically derived from lognormal functions fitted to the track distributions of the blanks and the control urines. The mathematically-derived cumulative distributions are seen to fit and characterize well the actual distribution of interpreted results, either for the case of the "well-known blank" (subtraction of a constant average blank output) or for the case where a "paired blank" having the distribution in Figure 6 is subtracted to obtain each result. A rigorous derivation (11, 12) of the mathematical forms of the interpreted distributions is not possible here, but for its possible application to

many situations where small or negative results are prevalent (either for discrete count data or continuous exposure measurements), a summary of the basic formulations are given in the following paragraphs.

The linear regression equation for the FTA calibration line, relating the output X in attocuries to the fission tracks Y will be of the form:

$$Y = mX + b \qquad \text{Eq. 10}$$

The values of m and b can be obtained from weighted or simple linear regression. For interpreting results in numbers of tracks observed for human urine samples, Equation 10 is used in reverse, i.e., to obtain an activity x_j in aCi per standard volume of a daily sample from a given number of observed tracks y_j. However, since different volumes of urine are turned in, and different size aliquots of the digested volumes may be used, a "scaling factor" f_j must be used as a multiplier of y_j. Thus, for interpretation of human samples, the interpreted one-day excretion of plutonium in a given urine sample is obtained as:

$$x_j = (y_j f_j - b)/m \qquad \text{Eq. 11}$$

The probability density functions, fitted using the maximum likelihood estimators for geometric mean and standard geometric deviation, for the fy and b distributions are derived to be (12):

$$p_{fy}(u) = (1/\sigma_{g,fy}\sqrt{2\pi})(1/u)\exp[-(\ln u - \ln \mu_{g,fy})^2/2\sigma_{g,fy}^2], \qquad \text{Eq. 12}$$

where the maximum likelihood parameters are $m_{g,fy} = 32$, and $s_{g,fy} = 0.727$; and.

$$p(b)db = (1/\sigma b\sqrt{2\pi})(1/b)\exp[-(\ln b - \ln \mu_{gb})^2/2\sigma b^2\, db, \qquad \text{Eq. 13}$$

where $\mu_{gb} = 15.93$ and $\sigma b = 0.656$. Using the regression value of m = 1.073, deriving the pdf for the fy/m distribution, $pw(w)\, dw = (1/\sigma_{g,fy}\sqrt{2\pi})(1/w)\exp[-(\ln mw - \ln \mu_{g,fy})^2/2\sigma_{g,fy}^2\, dw$, and a series of other transformations and algebraic manipulations of inequalities, the following analytic forms for the cumulative distribution functions used to obtain the theoretical points in Figure 8 became (12):

$$F_x(X) = \int_{w\to 0}^{w=X+(b/m)} (1/\sigma_{g,fy}\sqrt{2\pi})(1/w)\exp[-(\ln mw - \ln \mu_{g,fy})^2/2\sigma_{g,fy}^2]\, dw, \qquad \text{Eq.14}$$

for the case of the constant blank value b; and

$$F(X) = \int_{\varepsilon}^{B} p(b) \left\{\int_{\varepsilon}^{X+(b/m)} pw(w)\, dw\right\} db, \qquad \text{Eq. 15}$$

for the case of the paired random blank, where the value of e for the lower limit of integration of each integral must be close enough to zero for convergence of the integration, and the upper limit B of the integration over db must be high enough to include the range over which the probability is very close to 1 of obtaining a value of b. These forms of F(X) were used to obtain the theoretical points in Figure 8 that fitted the distribution of observed results.

Although the FTA track data might be expected to be better represented by a discrete pdf, it turns out that the smearing of discrete values by continuously fluctuating sources of uncertainty (such as chemical yields) makes the fy and b distributions essentially perfect lognormal distributions. This type of analysis helped the author understand why other data in the literature, such as the many tissue analyses presented by McInroy *et al.*(20), also tended to curve toward minus infinity in concentration values. (Minus infinity can not be reached on a logarithmic scale; but the distribution must lean toward much smaller values in the low concentration region.) Now that an analytical method is available to characterize the actual distributions of analytical results, these analytical distribution functions for interpreted results can be used for deriving statistical decision levels and tests of differences in populations, without the need to assume (often erroneously) normal, lognormal, or other distributions.

Response vs. Dose Distributions (Independent Points)

Distributions of response vs. dose (often called "dose-response" relationships) differ from those described in the previous section, in that the data points are each independently derived from separate groups of exposed humans or animals, the effects for each corrected by a stochastically independent subtraction of the effects for, e.g., the same age and sex standardized and matched population. (In some cases, controls have not been properly independent (12)). Finney (13) described in detail the mathematical theory and practical use of the lognormal function in "probit analysis" of toxicologic data. The lognormal type of plot has been used

extensively in examining toxic response ("quantal response"). The appearance of two parallel lines on the lognormal scale indicated that two agents or drugs affected animals by the same mechanisms of toxicity, the ratio of doses at each level then becoming the "relative potency" of the two drugs" (analogous to the RBE in radiation biology).

Examples of lognormal dose-response relationships observed by the author are shown in Figures 9-12. These types of data may be fit by either appropriate regression analyses or by use of maximum likelihood estimation of parameters (13-15). A lognormal response relationship (an "s-shaped curve, usually, on linear-linear coordinates) can be interpreted in the cumulative distribution sense as indicating the percent of animals susceptible to doses equal to or lower than that indicated on the x (dose) axis.

In 1963 there was concern that astronauts might be exposed in space to high-energy protons that had very high RBEs. Figure 9 shows the two parallel lines obtained at the University of Pittsburgh (UP) for the lognormal responses of lethality of mice to 440 MeV protons compared to 125 Kvp x rays (1). Two nearly parallel lines, but with steeper slopes, were obtained by replotting University of California data for 730 MeV and 250 Kvp x rays. The parallel appearance on this scale indicates similarity of the biological response mechanisms between very high energy protons and x rays, but differing potencies. The steeper slopes of the UC data are indicative of a purer animal strain than the UP mice descended from a cross of four in-bred strains (1).

Figures 10 and 11 show examples (8) of lognormal distributions of lung tumor incidence in rats from two different beta-emitting nuclides (22,23), and of human bone sarcomas vs. the internal alpha dose to bone (24,25). Figure 12 shows that, when converted to excess absolute risk, solid cancer mortality among Japanese atomic bomb survivors also exhibits the lognormal shape (10). Unexpected, this latter plot was also nearly linear on a linear-linear plot, the upward curvature indicated by the positive second derivative of the lognormal function becoming slightly evident only below about 1 rad. A two-sequential-stage model of carcinogenesis, not based on any empirical assumptions but derived analytically from certain chemical carcinogenesis data, follows the lognormal dose-response shape so closely that it raises the question of whether the lognormal appearance of responses might result from only two statistically-dominant events, rather than a chain of multiplicative variates as in the case of the cumulative concentration data (8-10). The literature has many more examples of lognormal responses.

It is difficult to understand why the lognormal function is so rarely used in radiobiology.

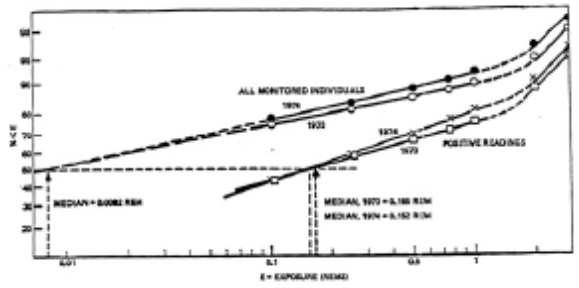

Figure 1. Probability-log scale plot of cumulative doses of U. S. licensee employees, 1973-74 (Reference 7)

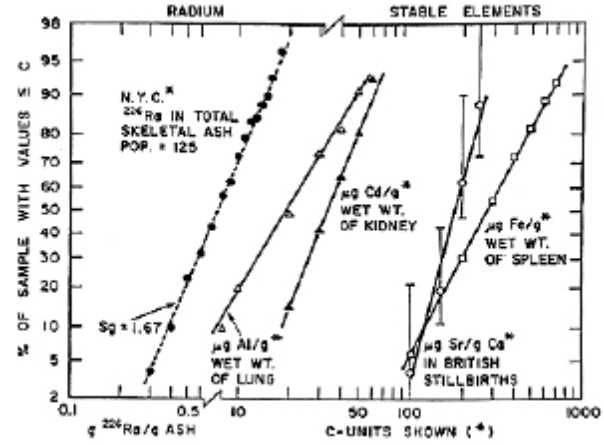

Figure 2. Cumulative distributions of natural element concentrations in human tissue samples (adapted from Figure 3, Reference 4)

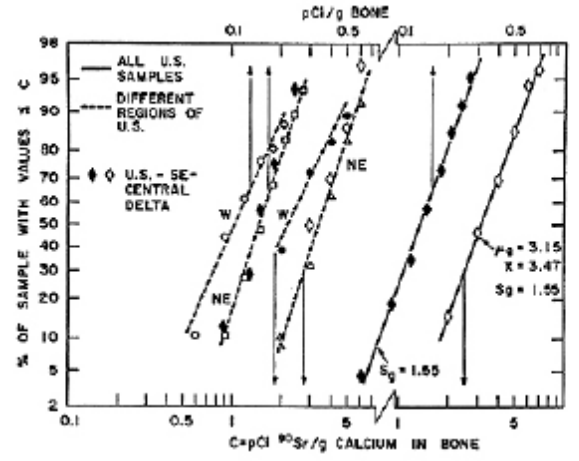

Figure 3. Cumulative distributions of ^{90}Sr in U. S. bone samples, 1964-65 (adapted from Figure 5, Reference 4)

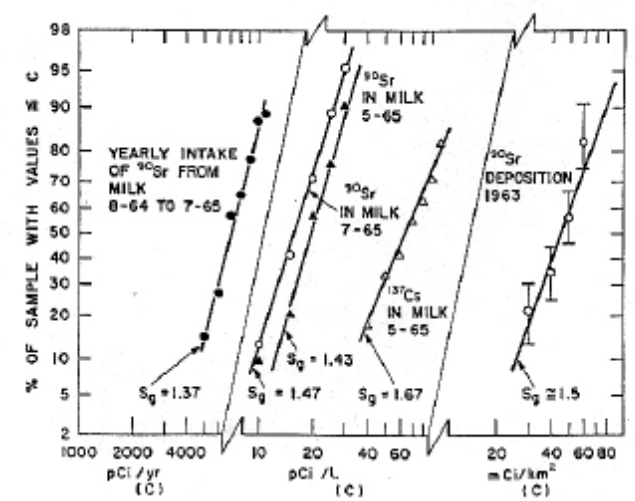

Figure 4. Deposition of ^{90}Sr and intakes of ^{90}Sr and ^{137}Cs in milk, USA, 1963-65 (adapated from Figure 6, Reference 4)

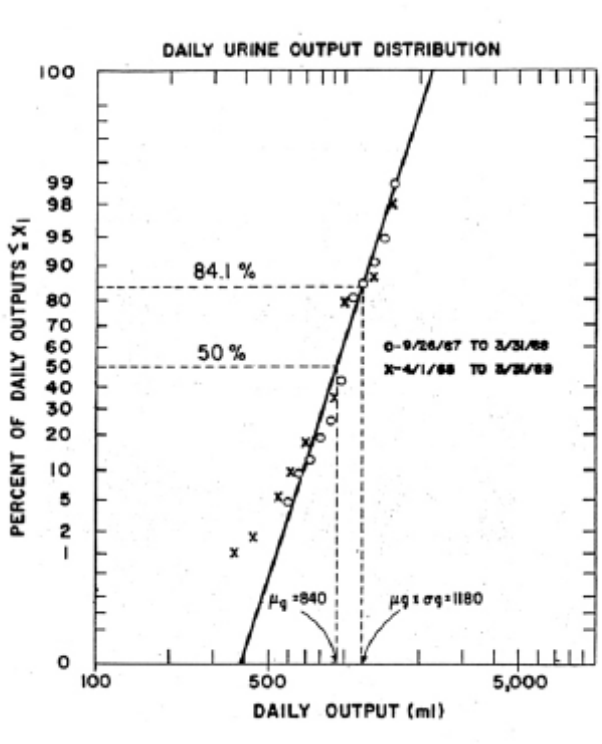

Figure 5. Distribution of daily urinary output volumes of ^{241}Am worker under chelation therapy (Reference 5)

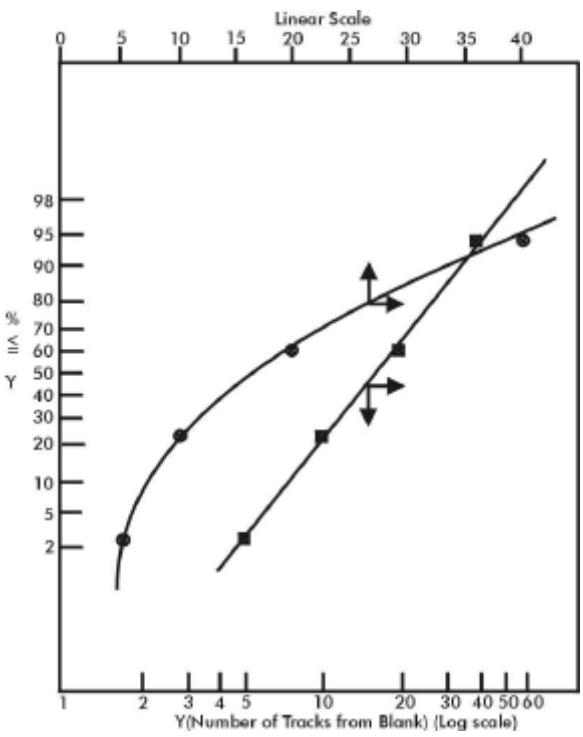

Figure 6. Distribution of simulated urine blank tracks in fission track analysis (FTA) of Pu in urine (References 11, 12)

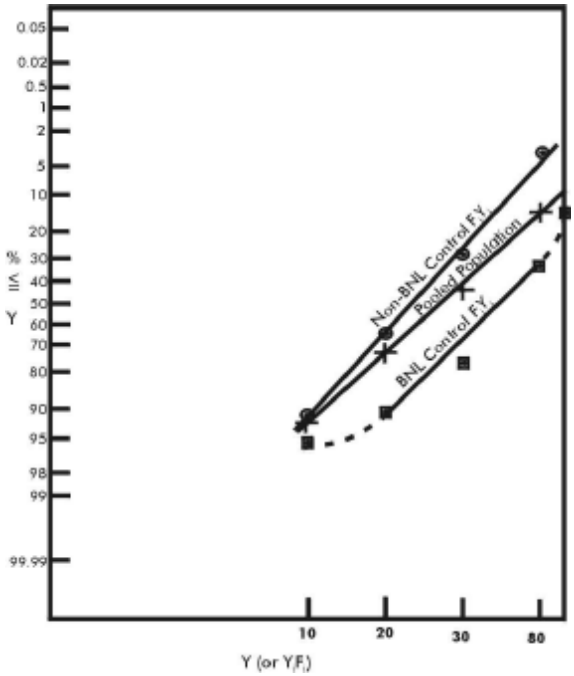

Figure 7. Distribution of tracks from control population urines in FTA analysis of Pu in urine (References 11, 12)

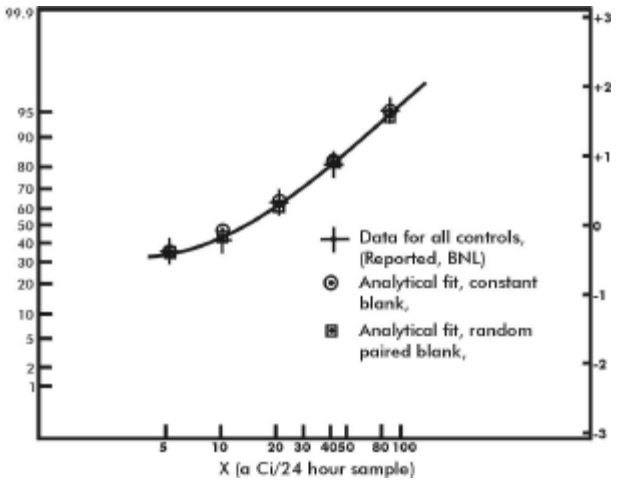

Figure 8. Distribution of interpreted activities of Pu in control population urine, after subtracting random blanks or a mean blank value (References 11, 12)

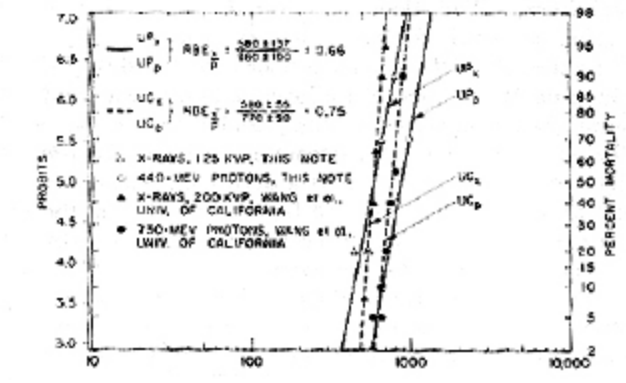

Figure 9. Response vs. dose for producing lethality in mice with 440- and 730-MeV protons (adapted from Reference 1)

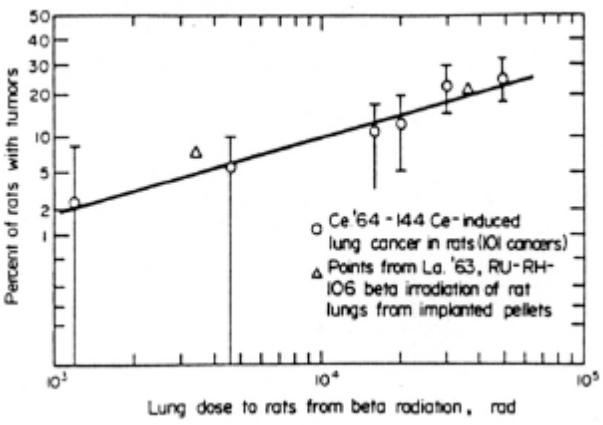

Figure 10. Lung tumor incidence in rats vs. internal dose for ^{144}Ce-Pr and ^{106}Ru-Rh (adapted from Figure 4, Reference 8)

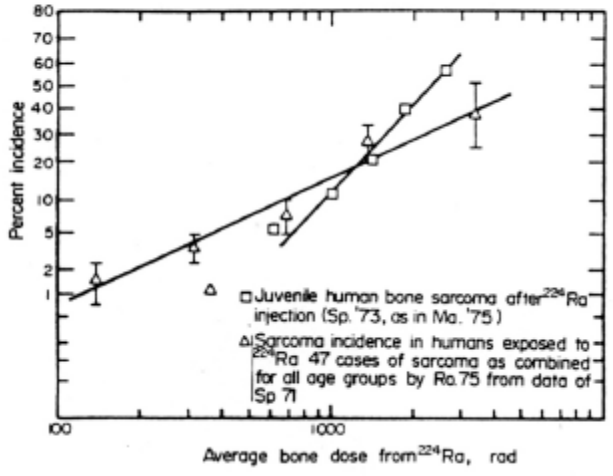

Figure 11. Human bone sarcomas vs. lifetime internal bone dose from ^{224}Ra (adapted from Figure 4, Reference 8)

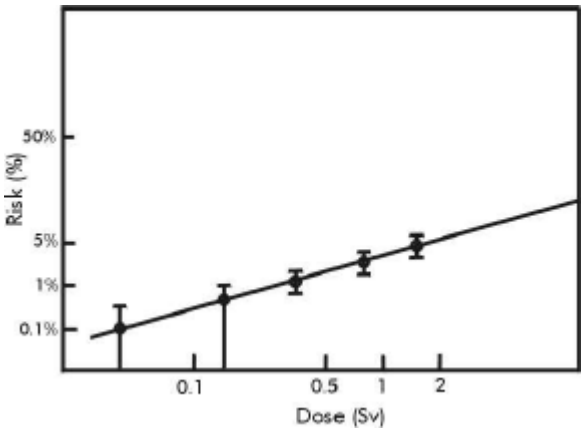

Figure 12. Excess absolute risk of solid cancers vs. dose for Japanese atomic bomb survivors (from Reference 10)

REFERENCES

1. F. J. Bradley, J. A. Watson, D. P. Doolittle, A. Brodsky and R. B. Sutton, *RBE of 440-MeV Proton Radiation Compared to 125 Kvp X-Rays for LD 50(30) of Mice*. Health Phys. 10, 71-74 (1964).
2. A. Brodsky, A. McNight, N. Wald and R. J. Catlin, *Cumulative Occupational Exposure Distributions in an Atomic Energy Facility*. Health Phys. 10(8), 163 (1964).
3. A. Brodsky, *A Stochastic Model of Carcinogenesis and its Implications in the Dose-Response Plane*. Health Phys. 8, 1176 (1966).
4. J. Schubert, A. Brodsky and S. Tyler, *The Log-Normal Function as a Stochastic Model of the Distribution of Sr-90 and Other Fission Products in Humans*. Health Phys. 13, 1187-1204 (1967).
5. A. Brodsky, N. Wald, I. S. Horm and B. J. Varzaly, *The Removal of Am-241 from Humans by DTPA*. Health Phys. 17, 379 (1969).
6. R. P. Specht and A. Brodsky, *Log-Normal Distributions of Occupational Exposure to Medical Personnel*. Health Phys. 31, 160-162 (1976).
7. A. Brodsky, R. P. Specht, B. Brooks and W. S. Cool, *Log-Normal Distributions of Occupational Exposure in Medicine and Industry.* In P. L. Carson, W. R. Hendee and D. C. Hunt, editors, *Occupational Health Physics*. Central Rocky Mountain Chapter, Health Physics Society, P. O. Box 3229, Boulder, CO 80303 (1976).
8. A. Brodsky, *A Stochastic Model of Carcinogenesis Incorporating Certain Obserations from Chemical and Radiation Dose-Response Data*. Health Phys. 35, 421-428 (1978).
9. A. Brodsky, *Time and Dose Factors in Carcinogenesis*. Health Phys. 36, 468-471 (1979).
10. A. Brodsky, *Dose-Response Shapes: Linear Excess Relative Risk or Lognormal Excess Absolute Risk*. Health Phys. 74(6), supplement, S50-S51 (1998).
11. A. Brodsky, D. M. Schaeffer, S. O'Toole, E. Kaplan, N. Barss, J. Dancz, W. J. Klemm, D. A. Raine III and J. Stiver, *Statistical Model for Fission Track Analysis of Plutonium in Human Samples*. Health Phys. 76(6), S175 (1999).
12. A. Brodsky and N. M. Barss, *Mathematically Analytic Distributions to Fit Radioanalytic Results*. Poster presented at the 45th Conference on Bioassay, Analytical and Environmental Radiochemistry, National Institue of Standards and Technology, Gaithersburg, MD (October 18-22, 1999). (Available from author.)
13. D. J. Finney, *Probit Analysis: a Statistical Treatment of the Sigmoid Response Curve, 2nd Edition*. Cambridge University Press, London (1952).
14. J. Aitchison and J. A. C. Brown, *The Lognormal Distribution, with special reference to its uses in economics*. Cambridge University Press, London (1963).
15. R. O. Gilbert, *Statistical Methods for Environmental Pollution Monitoring*. Van Nostrand Reinhold Company, New York (1987).
16. T. Hatch and S. P. Choate, *Statistical Description of the Size Properties of Non-Uniform Particulate Substances*. J. Franklin Inst. 207, 369 (1929).
17. T. Hatch, *Determination of 'Average Particle Size' from the Screen-Analysis of Non-Uniform Particles*. J. Franklin Inst. 215, 27 (1933).
18. A. Brodsky, *Statistical Methods of Data Analysis*. In A. Brodsky, Editor, *Handbook of Radiation Measurement and Protection, Section A, Vol. II: Mathematical and Biological Information*. CRC Press, Inc., Boca Raton, Florida (1982).
19. W. N. Sont, *A Summary of Data on Accumulated Occupational Radiation Doses Among Canadian Workers*. Health Phys. 67(4),393-398 (1994).
20. J. F. McInroy, E. E. Campbell, W. D. Moss, G. L. Tietgen, B. C. Eutsler and H. A. Boyd, *Plutonium in Autopsy Tissue*. Health Phys. 37, 1-136 (1979).
21. A. Brodsky, *Review of Radiation Risks and Uranium Toxicity*. RSA Publications, Hebron, Connecticut, USA (1996), pp. 90-92.
22. H. Cember, *Empirical Establishment of Cancer-Associated Dose to the Lung from ^{144}Ce*.Health Phys. 10, 1177-1180 (1964).
23. S. Laskin, M. Kuschner, N. Nelson, B. Altshuler, J. Harley and M. Daniels, *Carcinoma of the Lung in Rats Exposed to the Beta Radiation of Intrabronchial Ruthenium-106 Pellets*. J. Natn. Cancer Inst. 31, 219 (1963).
24. C. W. Mays, H. Spies, G. N. Taylor, R. D. Lloyd, W. S. S. Jee, S. S. McFarland, D. H. Taysuma, T. W. Brammer, D. Brammer and T. A. Pollard, *Estimated Risk to Human Bone from ^{238}Pu*. In W. S. S. Jee, Editor, *Health Effects of Plutonium and Radium*. J. W. Press, Salt Lake City, Utah, USA (1975), p. 351.
25. R. E. Rowland, *The Risk of Malignancy from Internally-Deposited Radioisotopes*. In O. F. Nygard, H. I. Adler and W. K. Sinclair, Academic Press, New York, USA (1975), pp.146-149.